A Generalization of the Fourier Transform and its Application to Spectral Analysis of Chirp-like Signals

Mamadou Mboup, Tülay Adali

A Generalization of the Fourier Transform and its Application to Spectral Analysis of Chirp-like Signals

Mamadou Mboup[a,*], Tülay Adalı[b]

[a]*Université de Reims Champagne Ardenne, CReSTIC- UFR des Sciences Exactes et Naturelles, Moulin de la Housse BP 1039, 51687 Reims cedex 2, France*
[b]*University of Maryland Baltimore County, Baltimore, Maryland 21250, USA*

Abstract

We show that the de Branges theory provides a useful generalization of the Fourier Transform (FT). The formulation is quite rich in that by selecting the appropriate parametrization, one can obtain spectral representation for a number of important cases. We demonstrate two such cases in this paper: the finite sum of elementary chirp-like signals, and a decaying chirp using Bessel functions. We show that when defined in the framework of de Branges spaces, these cases admit a representation very much similar to the spectral representation of a finite sum of sinusoids for the usual FT.

Keywords: de Branges spaces, Fourier transform, chirps, reproducing kernel

1. Introduction

Harmonic analysis, in particular the Fourier Transform (FT), plays a key role in many science and engineering disciplines including signal processing. Besides other alternatives such as the wavelet analysis [1] or the Wigner-Ville distribution [2], there are also a number of generalizations of the FT such as the fractional FT [3] and the short-time FT, to address cases where the structure of the signal does not allow an easy representation in terms of complex sinusoids. In this letter, we introduce a generalization of Fourier analysis developed by de Branges at the end of the sixties [4] and demonstrate its application to analysis of chirp-like signals as an example (see *e.g.* [2], [5], [6], [7]).

The main developments from the de Branges theory that will be needed are reviewed in a short summary in the next section. We then introduce a key theorem that allows for a very rich class generalization of the FT. In Section 3, we demonstrate an example of particular interest, analysis of exponential chirp signals and demonstrate simulation examples including the linear and the frequency-modulated chirps. A new class of chirps is introduced in section 4. These, subsequently called Bessel chirp, can also be interpreted in terms of generalized Hankel transform.

☆This work was partially supported by the NSF grant NSF-CCF 0635129.
*Corresponding author
Email addresses: Mamadou.Mboup@univ-reims.fr (Mamadou Mboup), adali@umbc.edu (Tülay Adalı)

2. Preliminaries

Let $\mathcal{H}$ be a Hilbert space of functions defined on a set $\Omega \subset \mathbb{C}$. If the point evaluation functional $w \mapsto F(w)$ is continuous, then this element of the continuous dual is represented by a single function $\mathcal{K}(w, \cdot)$ such that

1. $\mathcal{K}(w, z) \in \mathcal{H}$, $\forall\, w \in \Omega$;
2. $F(w) = \langle \mathcal{K}(w, z), F(z) \rangle$, $\forall\, F \in \mathcal{H}$, $\forall w \in \Omega$.

Then, $\mathcal{H}$ is called a reproducing kernel Hilbert space (RKHS), with reproducing kernel $\mathcal{K}$. A well-known example of a RKHS is the Paley-Wiener space (see *e.g.* [8]), which is the image of the set of bandlimited signals $f \in L_2(-\infty, \infty)$ with $\mathsf{supp}(f) \subset [-\tau, \tau]$, by

$$F(z) = \frac{1}{2\pi} \int_{-\infty}^{\infty} e^{izt} f(t) dt. \tag{1}$$

Any such F is an entire function of exponential type at most τ and square integrable on the real line and vice versa. The associated reproducing kernel is given by the transform of $\mathbb{1}_{[-\tau, \tau]}(\lambda) e^{-i\lambda\overline{w}}$, *i.e.*,

$$\mathcal{K}(w, z) = \frac{1}{2\pi} \int_{-\tau}^{\tau} e^{-i\lambda\overline{w}} e^{i\lambda z} d\lambda = \frac{\sin\{\tau(\overline{w} - z)\}}{\pi(\overline{w} - z)} = \frac{\tau}{\pi} \operatorname{sinc}\{\tau(\overline{w} - z)\}. \tag{2}$$

The Paley-Wiener theory has many implications in signal processing and it has been extended in various directions [9], [10], [11]. The de Branges's theory is one such generalization. In what follows, we present the application of the de Branges theory to the spectral analysis of chirp-like signals.

The Hilbert space theory of entire functions is due to de Branges [4] who developed a generalization of the Fourier analysis at the end of the sixties. Following [12], the main ingredients may be summarized as follows. Consider the matrix-valued function,

$$\mathfrak{m}(t) = \begin{pmatrix} \alpha(t) & \beta(t) \\ \beta(t) & \gamma(t) \end{pmatrix} \tag{3}$$

where $\alpha(t), \beta(t)$, and $\gamma(t)$ are absolutely continuous real functions such that[1] $\alpha'(t) > 0$ and $\gamma'(t) > 0$ and $\alpha'(t)\gamma'(t) - \beta'(t)^2 > 0$ for all $t > 0$. Here, we use the notation $u'(t) \stackrel{\triangle}{=} \frac{d}{dt} u(t)$. For each complex number z, we denote by $\boldsymbol{X}(t, z) \stackrel{\triangle}{=} \begin{bmatrix} A(t, z) \\ B(t, z) \end{bmatrix}$ the unique solution of the Cauchy problem

$$\begin{cases} \frac{d}{dt} \boldsymbol{X}(t, z) = z \boldsymbol{J} \mathfrak{m}'(t) \boldsymbol{X}(t, z) \\ \boldsymbol{X}(0, z) = \begin{bmatrix} 1 \\ 0 \end{bmatrix} \end{cases} \quad \text{where } \boldsymbol{J} = \begin{pmatrix} 0 & -1 \\ 1 & 0 \end{pmatrix}. \tag{4}$$

For each fixed $t > 0$, $A(t, z)$ and $B(t, z)$ are entire functions of z, real for z real. Let us now define the function

$$\mathcal{E}(t, z) = A(t, z) - \frac{i}{\sqrt{\alpha'(t)\gamma'(t) - \beta'(t)^2}} \left(\beta'(t) A(t, z) + \gamma'(t) B(t, z) \right) \quad \text{for } t > 0, \tag{5}$$

[1] We restrict here the theory to the case where $\mathfrak{m}'(t)$ is postive definite.

that we extend for negative t by setting $\mathcal{E}(-t,z) \stackrel{\triangle}{=} \overline{\mathcal{E}(t,\overline{z})} \stackrel{\triangle}{=} \mathcal{E}^*(t,z)$.

Theorem 1 (De Branges spaces [4]). *Let $\sigma(t) = \alpha'(t) - \frac{\beta'(t)^2}{\gamma'(t)}$ and $\sigma(-t) \stackrel{\triangle}{=} \sigma(t), t > 0$. Then we have:*

1. *For each fixed $\tau > 0$ the set $\mathcal{H}\{\mathcal{E}(\tau,z)\}$ of functions*

$$\widehat{f}_\tau(z) = \frac{1}{2\pi}\int_{-\tau}^{\tau} f(t)\mathcal{E}(t,z)\sigma(t)dt, \tag{6}$$

   where $f \in L_2(\mathbb{R},\sigma(t)dt)$ with $\mathsf{supp}(f) \subset [-\tau,\tau]$, is a RKHS of entire functions, with reproducing kernel

$$\mathcal{K}_\tau(w,z) = \frac{A(\tau,z)B(\tau,\overline{w}) - B(\tau,z)A(\tau,\overline{w})}{\pi(\overline{w}-z)}. \tag{7}$$

2. *There exists a unique nonnegative measure μ on the Borel sets of the real line such that $\mathcal{H}\{\mathcal{E}(a,z)\}$ is contained isometrically in $L_2(d\mu)$.*

3. *The Parseval equality*

$$\|\widehat{f}_\tau(\cdot)\|^2_{\mathcal{H}\{\mathcal{E}\}} = \int |\widehat{f}_\tau(x)|^2 d\mu(x) = \frac{1}{2\pi}\int_{-\tau}^{\tau} |f(t)|^2\sigma(t)dt = \|f\|^2_\sigma \tag{8}$$

   holds and for any $f \in L_2(\sigma dt)$, the function defined on the real line by

$$\widehat{f}(x) = \frac{1}{2\pi}\int_{-\infty}^{\infty} f(t)\mathcal{E}(t,x)\sigma(t)dt, \tag{9}$$

   where the integral is to be understood as $\lim_{c\to\infty}\int_{-c}^{c}$, exists in the metric of $L_2(d\mu)$ and (8) *holds. Every element of $L_2(d\mu)$ is of this form.*

With $\mathfrak{m}(t) = t\mathbf{I}$ where $\mathbf{I}$ is the identity matrix, we obtain $\mathcal{E}(t,z) = e^{-izt}$, $\sigma(t) \equiv 1$. Then $\mathcal{H}\{\mathcal{E}(a,z)\}$ reduces to the classical Paley-Wiener space and (9) is simply the Fourier transform.

We use the given generalized Fourier transform for spectral analysis of chirp signals (see [2] for a clear-cut definition). We first consider exponential-like chirp signals. Next we introduce the Bessel-chirp signals.

3. Spectral analysis of exponential chirp signals

For $\tau > 0$, let us consider the de Branges space $\mathcal{H}\{\mathcal{E}(\tau,z)\}$ built from the choice $\mathfrak{m}(t) = \psi(t)\mathbf{I}$. As one may readily check, the corresponding solution of (4) leads to $\mathcal{E}(t,z) = e^{-i\psi(t)z}$ with $\sigma(t) = \psi'(|t|)$. The transform (6) then reads as

$$\widehat{f}_\tau(z) = \frac{1}{2\pi}\int_{-\tau}^{\tau} f(t)e^{i\psi(t)z}\psi'(|t|)dt. \tag{10}$$

This decomposition reminds one the so-called *chirplet* transform [13],[5], [6] although there are significant differences. For instance, we will see in §3.1.1 that the transform of

an elementary chirp tends to a Dirac pulse (when $\tau \to \infty$) as opposed to the chirplet transform. Also, the atoms of the decomposition given here are as simple as possible as shown by the following examples, which can be compared to, *e.g.* those in [7], [14] that involve four parameters for the chirplet:

$$\psi(t) = \begin{cases} t^2 & \text{linear chirp,} \\ t + \beta \sin(t) & \text{frequency modulation, with index } 0 < \beta \leqslant 1 \end{cases}$$

Let $\mathcal{K}_\tau(w, z)$ denote the reproducing kernel of $\mathcal{H}\{\mathcal{E}(\tau, z)\}$ and recall that the set $\mathcal{M}$ of functions of the form $F(z) = \sum_k \alpha_k \mathcal{K}_\tau(w_k, z)$ where $\alpha_k, w_k \in \mathbb{C}$, is dense in $\mathcal{H}\{\mathcal{E}(\tau, z)\}$. Hence, since $\mathcal{K}_\tau(w, z)$ can also be identified by the transform (10) of $\overline{\mathcal{E}(\cdot, w)}$ (see [15]), we have:

$$F(z) = \frac{1}{2\pi} \sum_k \alpha_k \int_{-\tau}^{\tau} \overline{\mathcal{E}(t, w_k)} \mathcal{E}(t, z) \psi'(t) dt, \tag{11}$$

$$= \frac{1}{2\pi} \int_{-\tau}^{\tau} \varphi(t) \mathcal{E}(t, z) \psi'(t) dt = \widehat{\varphi}_\tau(z). \tag{12}$$

Hence, we may identify $\mathcal{M}$ as the transforms of elements of the form

$$\varphi(t) = \sum_k \alpha_k \overline{\mathcal{E}(t, w_k)}, \quad t \in [-\tau, \tau] \tag{13}$$

Before closing this section, note that with $\mathcal{E}(t, z) = e^{-i\psi(t)z}$, the reproducing kernel (7) of $\mathcal{H}\{\mathcal{E}(\tau, z)\}$ is readily given by:

$$\mathcal{K}_\tau(w, z) = \frac{\sin\{\psi(\tau)(\overline{w} - z)\}}{\pi(\overline{w} - z)} = \frac{\psi(\tau)}{\pi} \operatorname{sinc}\{\psi(\tau)(\overline{w} - z)\}, \tag{14}$$

where we recover (2) as expected since we still consider *bandlimited* signals.

3.1. Spectrum lines and linear chirp parameter estimation

As is well known, the spectrum of a finite sum of sinusoids is composed of separate spectrum lines corresponding to different sinusoids. We show that the same holds true with a finite sum of chirp-like signals provided the spectrum is defined in the framework of de Branges spaces. Chirp parameter estimation is therefore possible following the same lines as frequency estimation (see also [16] for estimation based on fast chirp transform or [17] for time-frequency or [18] for time-scale approaches).

To simplify the presentation, without any loss of generality, we consider the linear chirp case. The corresponding function $\psi(t)$ is then given by the second order monomial $\psi(t) = t^2$. With $w_k = \theta_k + i\lambda_k$, the elements $\varphi(t)$ in (13) can be written as

$$\varphi(t) = \sum_k \alpha_k e^{-it^2\theta_k} e^{-t^2\lambda_k}, \quad \text{for } t \geqslant 0. \tag{15}$$

In the sequel, we consider only real values for w_k but with a general second-order polynomial for ψ_k and also we take into account the presence of noise. So, let $y(t)$ be a noisy sum of linear chirp signals as in

$$y(t) = \sum_{k=0}^{N} \alpha_k e^{-i\psi_k(t)} + b(t), \tag{16}$$

where $\psi_k(t) = \theta_k t^2 + \rho_k t + \eta_k$, for $k = 0, \ldots, N$ and $b(t)$ is the additive noise term. We consider the estimation of the parameters $\theta_k, \rho_k, \eta_k, \alpha_k$, $k = 0, \ldots, N$, based on the measurement $y(t)$. A similar estimation problem is studied in [14] (see also [13], [5], [6]) for chirplet decomposition, and in [19], both using a maximum likelihood approach (see also [20] that uses a least squares method).

3.1.1. Elementary Chirp

Let us first begin with the simple case of a single chirp $s(t) = \alpha e^{-i\psi(t)}, t \geqslant 0$, with $\psi(t) = \theta t^2$. Because this signal also reads as $s(t) = \overline{\mathcal{E}(t, \theta)}$, its transform is given by

$$\widehat{s}_\tau(z) = \alpha \mathcal{K}_\tau(\theta, z). \tag{17}$$

Since the reproducing kernel is a sinc function, the parameters α and θ fulfill

$$\theta = \arg\max_{\xi \in \mathbb{R}} |\widehat{s}_\tau(\xi)|, \tag{18}$$

$$\alpha = \frac{\pi}{\tau^2} \widehat{s}_\tau(\theta). \tag{19}$$

Moreover, observe that for $\xi \in \mathbb{R}$, $\mathcal{K}_\tau(\theta, \xi)$ is the classical Fourier transform of the indicator function $\mathbb{1}_{[-\psi(\tau),\, \psi(\tau)]}$. Then, noting $\delta(\cdot)$ the Dirac distribution, we have

$$\lim_{\tau \to \infty} \mathcal{K}_\tau(\theta, \xi) = \delta(\theta - \xi).$$

3.1.2. Multiple elementary Chirps

With a signal composed of several elementary chirps, as in $s(t) = \sum_k \alpha_k e^{-i\theta_k t^2}$, the preceding analysis shows that the parameters θ_k and α_k can be obtained from the maxima of $|\widehat{s}_\tau(\xi)|$. This is more apparent if, by invoking the preceding remark, we write

$$\lim_{\tau \to \infty} \widehat{s}_\tau(\xi) = \sum_k \alpha_k \delta(\theta_k - \xi).$$

3.1.3. General case

We now consider the more general case as described in (16). Each noise-free component is a translated version of an elementary chirp $s(t) = \widetilde{\alpha}\overline{\mathcal{E}(t, \theta)}$ upon setting

$$\alpha e^{-i(\theta t^2 + \rho t + \eta)} = \widetilde{\alpha}\overline{\mathcal{E}(t + r, \theta)} = s(t + r), \tag{20}$$

where $\widetilde{\alpha} = \alpha e^{-i\left(\eta - \rho^2/4\theta\right)}$ and $r = \frac{\rho}{2\theta}$. Note that the transform (6) is not translation invariant. So as $\widehat{f}_\tau(z)$ stands for the transform of $f(t)$ with $\mathsf{supp}(f) \in [-\tau, \tau]$, we introduce the notation $\widehat{F}_\tau(z, r)$ to represent the transform of $f(t + r)$. Let $\langle \cdot, \cdot \rangle$ be the inner product in $L_2([-\tau, \tau], \psi'(t)dt)$. The transform of $s(t + r)$ in (20) is thus:

$$\widehat{S}_\tau(z, r) = \langle \mathcal{E}(t + r, \theta), \mathcal{E}(t, z) \rangle. \tag{21}$$

The Cauchy-Schwartz inequality then shows that

$$(\theta, 0) = \arg\max_{(\xi, r) \in \mathbb{R}^2} |\widehat{S}_\tau(\xi, r)|. \tag{22}$$

The most general case where we allow $w_k = \theta_k + i\xi_k$ to live in the complex upper half plane, *i.e.* $\xi_k \geqslant 0$ in (15), can be handled with similar arguments.

The noise is assumed to have a covariance function satisfying: for all t_1, t_2, $\mathsf{E}(b(t_1)\overline{b(t_2)}) = C\delta(t_1 - t_2)$ for some constant $C > 0$. Then, for ω real, we obtain

$$\mathsf{E}|\widehat{b}_\tau(\omega)|^2 = \frac{1}{4\pi^2}\int_{-\tau}^{\tau}\int_{-\tau}^{\tau}\mathsf{E}(b(t_1)\overline{b(t_2)})\mathcal{E}(t_1,\omega)\overline{\mathcal{E}(t_2,\omega)}d\sigma(t_1)d\sigma(t_2) = \frac{C}{2\pi}\|\mathcal{K}_\tau(\omega,\cdot)\|^2.$$

3.2. Examples

3.2.1. Sum of linear chirps

Let z be fixed. For a given λ real, we compute the transform of $y(t+\lambda)$ using (10) *i.e.*, we calculate

$$\widehat{Y}_\tau(z,\lambda) = \frac{1}{2\pi}\int_{-\tau}^{\tau} y(t+\lambda)\mathcal{E}(t,z)|t|dt. \tag{23}$$

Assume that the signal $y(t)$ is causal, *i.e.* $y(t) = 0, \forall t < 0$ and define

$$h(t,z) = \begin{cases} -\mathcal{E}^*(t,z)t & 0 \leqslant t \leqslant \tau \\ 0 & \text{else.} \end{cases}$$

Then, using the change of variable $t \to -t$ in (23), one may rewrite $\widehat{Y}_\tau(z,\lambda)$ as the convolution

$$\widehat{Y}_\tau(z,\lambda) = \frac{1}{2\pi}\int_0^{\lambda} y(\lambda - t)h(t,z)dt. \tag{24}$$

We turn now to the discrete-time setting where only time samples of the observation, $y_m = y(t_m)$, are available. We assume a uniform sampling, $t_m = mT_s, m = 0,1,\ldots$, with sampling period T_s. Let $\tau = MT_s$: increasing M improves the resolution as in the classical Fourier analysis. Set $\lambda = nT_s$ and for z fixed, compute the finite sequence $\{h_m(z) \stackrel{\triangle}{=} T_s h(t_m,z)\}_{m=0}^M$. Then, by a numerical integration method with abscissas t_m and weights W_m, $m = 0,\cdots,M$, we obtain the approximation of (24):

$$\widehat{Y}_\tau(z,\lambda) \approx \sum_{m=0}^{M} W_m h_m(z) y_{n-m}.$$

In all the sequel, we use the trapezoidal method for which $W_0 = W_M = 0.5$, and $W_m = 1, m = 2,\cdots,M-1$. As $\lambda = nT_s$ varies, the sequence $\{\widehat{Y}_\tau(z,\lambda)\}$ reads as the output of the FIR filter with impulse response sequence $\{g_m(z) = W_m h_m(z)\}_{m=0}^M$ with z fixed.

We simulate a signal of the form (16), with $N = 2$. The parameters θ_k and r_k of the polynomial phase functions $\psi_k(t) = \theta_k t^2 + \rho_k t + \eta_k = \theta_k(t + r_k)^2 + \widetilde{\eta}_k$ and the amplitudes α_k, $k = 0,1,2$, chosen in this example are given in the following vectors, by: $\boldsymbol{\theta} = [2\pi/5,\ 2.2\pi/5,\ 4\pi/5]$, $\boldsymbol{r} = [28,\ 16.9,\ 4.6]T_s$ and $\boldsymbol{\alpha} = [2.3,\ 1.7,\ 1.8]$, where the sampling period is $T_s = 0.01$. Since the values of η_k are not relevant, we set $\widetilde{\eta}_k = 0$ throughout. We simulate a complex (circular) zero-mean white Gaussian noise sequence for $b(t_m)$, with a signal to noise ratio (SNR) of -5 dB.

We directly verify that the transform (23) is a linear combination of terms like $\widehat{S}_\tau(z,\lambda - r)$ in (21), plus the noise contribution. Now we know from (22) that the modulus of each

of these terms attains its maximum at $(z, \lambda - r) = (\theta_k, \lambda - r_k = 0)$. We therefore obtain the estimates of the parameters θ_k and r_k, or equivalently of ρ_k. This is illustrated in Figures 1 (a) and 2 where $|\widehat{Y}_\tau(\theta, \lambda)|$ is plotted as a function of θ and λ. Figure 1 (b) displays the projection of $|\widehat{Y}_\tau(\theta, \lambda)|$ to the plane $\lambda = 0$.

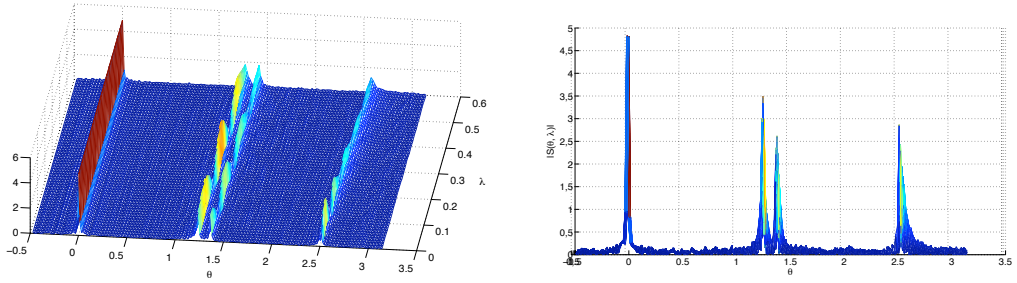

a) 3D view b) 2D projection

Figure 1: Spectrum of the linear chirp example

The three chirps are clearly recovered by the *spectral lines*. The noise is also represented by the spectral line at *frequency* $\theta = 0$. Its variance can be also read directly from the plot, in accordance with the Parseval equality (8).

Figure 2 shows the contour plot of the surface. The maxima of the surface provide

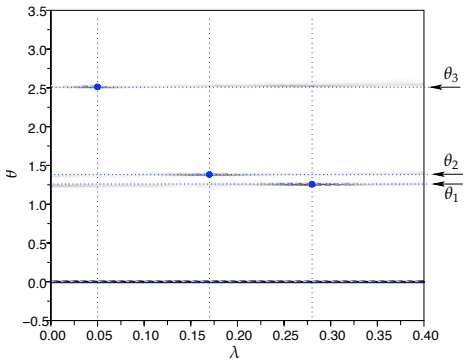

Figure 2: Contour plot of the spectrum for the linear chirp example

spectral estimation of the chirp parameters. These are indicated by the three big blue dots in the figure. The dotted line curves represent the original values of θ_k (horizontal) and r_k (vertical). For each k, the intersection of corresponding dotted lines coincides with the location of a local maximum.

3.2.2. Frequency-modulated chirp

In this example, we demonstrate the application of the steps given in Section 3.1.3 for the estimation of real parameters w_k and ξ_k of the decomposition:

$$y(t) = \sum_{k=0}^{N} \alpha_k e^{-iw_k(t+\frac{\beta}{\xi_k}\sin(\xi_k t))} = \sum_{k=0}^{N} \alpha_k \mathcal{E}^*\left(\xi_k t, \frac{w_k}{\xi_k}\right), \tag{25}$$

where the atoms are now sinusoidal chirps. This corresponds to the choice $\psi(t) = t + \beta\sin(t)$. Let us concentrate on a single term $s(t) = e^{-iw_0(t+\frac{\beta}{\xi_0}\sin(\xi_0 t))} = \mathcal{E}^*\left(\xi_0 t, \frac{w_0}{\xi_0}\right)$, $t \in [-\tau, \tau]$. The transform of $s(t/\xi)$, parametrized by $\xi > 0$, is

$$\begin{aligned}\widehat{S}_\tau(z,\xi) &= \frac{1}{2\pi}\int_{-\xi\tau}^{\xi\tau} \overline{\mathcal{E}\left(\frac{\xi_0}{\xi}t, \frac{w_0}{\xi_0}\right)}\mathcal{E}(t,z)\psi'(t)dt \\ &= \frac{\xi}{2\pi}\int_{-\tau}^{\tau} e^{i(\xi z - w_0)t} e^{i\beta(z\sin(\xi t) - \frac{w_0}{\xi_0}\sin(\xi_0 t))}(1+\beta\cos(\xi t))dt.\end{aligned} \tag{26}$$

Thus, the parameters w_0 and ξ_0 can be found from the global maximum of $|\widehat{S}_\tau(z,\xi)|$:

$$(w_0, \xi_0) = \arg\max_{(z,\xi)\in\mathbb{R}^2} |\widehat{S}_\tau(z,\xi)|.$$

However, the latter presents several local maxima. In particular, we obtain many spurious spectral lines corresponding, *e.g.* to $\xi z - w_0 = 0$, in addition to the horizontal line $z = \frac{w_0}{\xi_0}$. This is illustrated in Figure 3, which displays the contour plots of the modulus, $|\widehat{Y}_\tau(z,\xi)|$ for z real, of the transform of $y(t/\xi)$ in (25):

$$\widehat{Y}_\tau(z,\xi) = \frac{\xi}{2\pi}\int_{-\tau}^{\tau} y(t) e^{iz(\xi t + \beta\sin(\xi t))}(1+\beta\cos(\xi t))dt. \tag{27}$$

These results were obtained for $N = 2$ in (25) and the numerical values of the parameters w_k, ξ_k, α_k are given in the corresponding vectors $\boldsymbol{w} = [650,\ 680,\ 750]$, $\boldsymbol{\xi} = [81.5,\ 63,\ 51]$ and $\boldsymbol{\alpha} = [1.75,\ 0.87,\ -0.9]$. For the implementation we use a direct numerical integration to (27). As this example shows, the frequency estimation method described in Section 3.1 is not particularly suitable for all types of chirps.

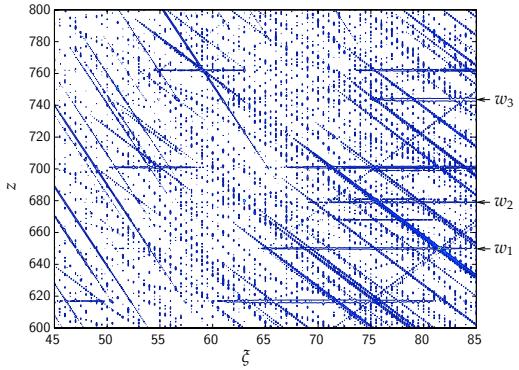

Figure 3: Contour plot of the spectrum for the frequency-modulated chirp example

4. The Bessel chirp and its spectral analysis

In this section, we introduce a new class of chirps where complex exponential is replaced by the Bessel functions $\mathcal{J}_\nu(z) = \sum_{n=0}^{\infty} \frac{(-1)^n (z/2)^{2n+\nu}}{n!\Gamma(\nu+n+1)}$. This class may be suitable, for instance, to model chirps with a decaying envelop. It is built from a matrix $\mathfrak{m}(t)$ in Theorem 1 of the form $\beta(t) = 0$, $\alpha(t) = \alpha_0 t^p$, $\gamma(t) = \gamma_0 t^{-q}$ for some $p, q > 0$. The de Branges theory then provides a corresponding generalization of the Fourier transform as given by the following theorem:

Theorem 2. *For $\nu > -1$, we define*

$$\mathcal{E}(t,z) = 2^{2\nu+1}\Gamma(\nu+1)(zt^2)^{-\nu}\left\{\mathcal{J}_\nu(zt^2) - i\mathcal{J}_{\nu+1}(zt^2)\right\}, \quad t \geqslant 0, \tag{28}$$

and $\mathcal{E}(-t,z) = \mathcal{E}^*(t,z)$. Then, for any fixed $\tau > 0$, the set of functions $\widehat{f}_\tau(z)$ that are images of functions $f \in L_2(|t|^{4\nu+3}dt)$ and vanish outside $[-\tau,\tau]$,

$$\widehat{f}_\tau(z) = \frac{1}{2\pi}\int_{-\tau}^{\tau} f(t)\mathcal{E}(t,z)\,|t|^{4\nu+3}dt \tag{29}$$

form a space $\mathcal{H}\{\mathcal{E}(\tau,z)\}$. The functions $\Phi_{\tau,n}(z) = \Gamma(\nu+1)(2\tau^2)^{2\nu+1}\left(\frac{\tau^2 z}{2}\right)^{-\nu}\frac{\mathcal{J}_{\nu+1}(\tau^2 z)}{z-\mathfrak{z}_{\nu,n}/\tau^2}$, where $\mathfrak{z}_{\nu,n}$ is the n^{th} zero of $\left(\frac{x}{2}\right)^{-\nu}\mathcal{J}_{\nu+1}(x)$, form a complete orthogonal set in $\mathcal{H}\{\mathcal{E}(\tau,z)\}$.

Proof. The function $\mathcal{E}(t,z)$ in (28) and hence the de Branges space $\mathcal{H}\{\mathcal{E}(\tau,z)\}$, follows from (4) in Theorem 1 upon setting $\alpha(t) = t^{4\nu+4}/(4^\nu(\nu+1))$, $\gamma(t) = -t^{-4\nu}/(4^{\nu+1}\nu)$ and $\beta(t) = 0$ in (3). Next, note that we also have $\Phi_{\tau,n}(z) = \frac{\mathcal{K}_\tau(\mathfrak{z}_{\nu,n},z)}{E(\mathfrak{z}_{\nu,n})}$ for some constant E depending on $\mathfrak{z}_{\nu,n}$. Their orthogonality follows from [4, Theorem 22], which also shows that $B(\tau,z)$ is the unique function orthogonal to all $\Phi_{\tau,n}(z)$. Now it is easy to verify that $B(\tau,z)$ does not belong to $\mathcal{H}\{\mathcal{E}(\tau,z)\}$ since $B(\tau,x)$ is not in $L_2(\mathbb{R},|x|^{4\nu+3}dx)$. □

Hence the integral in (29) represents a new generalization of the Fourier transform, where the complex exponential is replaced by a complex Bessel-like function. Another way to regard this integral is to consider $\widehat{f}_\tau(\cdot)$ to be a *chirp Hankel* transform of $f(t)$ since it is intimately related to the Hankel transform. Also, note that the orthogonality of the functions $\Phi_{\tau,n}(z)$, $n \in \mathbb{N}$ implies that the Kramer's sampling theorem [21], [22] holds here.

Now, we again use the settings of the numerical example in Section 3.2.1 where we replace the exponential chirp atoms by the Bessel chirp atom $\mathcal{E}(t,z)$ in (28) but use the same numerical implementation and values for the parameters.

In Figure 4, the contour plot of the surface $|\widehat{Y}_\tau(\theta,\lambda)|$, where (23) is replaced by its analog from (29), shows a very similar behavior to that of the linear chirp given in Figure 2: The three frequency components are clearly recovered with a distinct spectral line for each. The maxima of the surface are indicated by the three big dots in the figure. They coincide with the points (θ_k, r_k). The vertical dotted line curves represent the original values r_k.

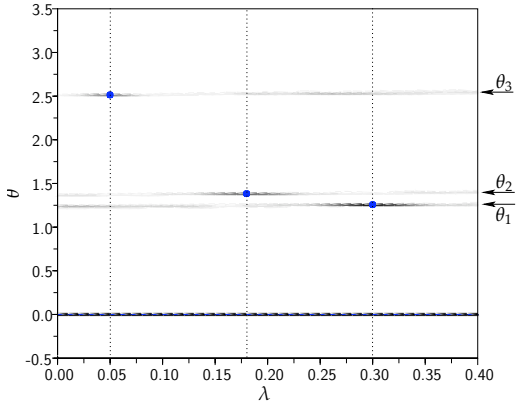

Figure 4: Contour plot of the spectrum for the Bessel chirp example

5. Conclusion

We present the de Branges's generalization of the Fourier transform and demonstrate its application for the spectral representation of chirp signals. In particular, we note that when defined within the de Branges framework, the representation is similar to that of sinusoids in that it is a sum of spectrum lines. In addition, we introduce a new type of chirp, the Bessel chirp, and present the generalization of the FT for this case.

In the example considered here, for the linear chirp, the representation may be seen as a warped version (change of variables: $t \to t^2$) [2] of the monochromatic waves in the regular Fourier analysis. This is immediate because a chirp atom is also a complex exponential function, though one with a more complex phase. However, such a warping interpretation does no longer hold in general since, unless $\mathfrak{m}(t)$ is a scalar function times a constant matrix, the atom of the decomposition is not an exponential function as can be seen with the Bessel-Chirp example. Therefore, by selecting $\mathfrak{m}(t)$ from a wide variety of possible forms, one can obtain very rich generalizations of the Fourier transform. Another interesting future topic is signal analysis using the Bessel chirp introduced in this paper, as it admits a rich and attractive way to represent real-world signals. Finally, a more efficient implementation would be desirable, *e.g.*, by using the techniques proposed in [16] for a fast chirp implementation.

References

[1] Y. Meyer, Wavelets and operators, Advanced mathematics. Cambridge University Press, 1992.
[2] P. Flandrin, Time-Frequency/Time-Scale analysis, Academic Press, San Diego, 1999.
[3] V. Namias, The fractional order fourier transform and its application to quantum mechanics, J. Inst. Appl. Math. 25 (1980) 241–265.
[4] L. De Branges, Espaces Hilbertiens de Fonctions Entières, Masson, Paris, 1972.
[5] S. Mann, S. Haykin, The chirplet transform: Physical considerations, IEEE Trans. Signal Processing 43 (11) (1995) 2745–2761.
[6] E. J. Candès, P. Charlton, H. Helgason, Detecting highly oscillatory signals by chirplet path pursuit, Appl. Comput. Harmon. Anal. 24 (2008) 14–40.
[7] A. Bultan, A four-parameter atomic decomposition of chirplets, IEEE Trans. Signal Processing 47 (1999) 731–745.

[8] W. Rudin, Real and complex analysis, McGraw-Hill, 1966.
[9] S. Saitoh, Generalizations of Paley-Wiener's theorem for entire functions of exponential type, Proceedings of the AMS 99 (3) (1987) 465–471.
[10] N. B. Andersen, Real Paley-Wiener theorems for the Hankel transform, Journ. of Fourier Anal. and Appli. 12 (1) (2006) 17–25.
[11] M. De Jeu, Paley-Wiener theorems for the dunkl transform, Transactions of the AMS 358 (10) (2006) 4225–4250.
[12] M. Mboup, On the structure of self-similar systems: A Hilbert space approach, in: Operator Theory: Advances and applications, Vol. OT-143, Birkhäuser-Verlag, 2003, pp. 273–302.
[13] S. Mann, S. Haykin, The chirplet transform: A generalization of Gabor's logon transform, in: Vision Interface '91, Canadian Image Processing and Patern Recognition Society, Calgary, Alberta, 1991, pp. 205–212.
[14] J. C. O'neill, P. Flandrin, W. C. Karl, Sparse representations with chirplets via maximum likelihood estimation, preprint (2000).
[15] S. Saitoh, Theory of reproducing kernels and its applications, Pitman Research Notes in Mathematics, Longman Scientic & Technical, UK, 1988.
[16] F. A. Jenet, T. A. Prince, Detection of variable frequency signals using a fast chirp transform, Phys. Rev. D 62 (2000) 122001.
[17] E. Chassande Mottin, P. Flandrin, On the time-frequency detection of chirps, Appl. Comput. Harmon. Anal. 6 (1999) 252–281.
[18] M. Morvidone, B. Torresani, Time scale approach for chirp detection, Int. J. Wavelets Multiresolut. Inf. Process. 1 (1) (2003) 19–49.
[19] S. Saha, S. M. Kay, Maximum likelihood parameter estimation of superimposed chirps using monte carlo importance sampling, IEEE Trans. Signal Processing 50 (2) (2002) 224–230.
[20] D. Kundu, S. Nandi, Parameter estimation of chirp signals in presence of stationary noise, Statistica Sinica 18 (1) (2008) 187–201.
[21] H. P. Kramer, A generalized sampling theorem, J. Math. Phys. 38 (1959) 68–72.
[22] A. I. Zayed, M. A. Shubov, Sampling theorem for bandlimited Hardy space functions generated by Regge problem, Appl. Comput. Harmon. Anal. 31 (2011) 125–142.